International Journal of Future Generation Communication and Networking
Vol. 13, No. 1, (2020), pp. 57-70

Rotationally Invariant Color, Texture and Shape Feature Descriptors for Image Retrieval

S.Sivakumar [1] and S.Sathiamoorthy [2*]

[1] *Division of Computer and Information Science, Annamalai Nagar India*
[2] *Tamil Virtual Academy, Chennai,*
[1] *sivassa77@gmail.com,* [2] *ks_sathia@yahoo.com*

Abstract

The incredible development in the number of digital images has aggravated the demand for step up in image retrieval. The prime challenge in image retrieval is retrieving akin images from huge image repositories with highest precision and least time and storage cost. Selecting apt feature descriptors plays noteworthy role in increasing the competence of retrieval systems for digital images. In this paper, integration of dominant rotation local binary pattern (DRLBP), dominant edgels (DE) and moments based on DEs, and dominant color descriptors (DCD) are proposed for image indexing and retrieval and are extracting texture, shape and color details respectively. Self-organizing map (SOM) is employed for classification which increases accuracy and decreases the search space considerably. In SOM, Manhattan distance is chosen as discriminant function. The competence of proposed system is evaluated by precision and retrieval time. The proposed system is tested on benchmark databases. The results obtained in the experiments provide evidence that there is a considerable improvement with proposed system when compare to existing systems for image retrievals. Manhattan measure is used to estimate the likeness between the images.

Keywords:*—LBP, Dominant LBP, Dominant edgels, Geometric shape features, Dominant color descriptor, Manhattan measure.*

1. Introduction

Rapid development in imaging equipment's raises the images in almost all domains such as entertainment, medicine, forensic science and geology. Since man-made annotations of images is cumbersome, expensive and time consuming work, content based image retrieval (CBIR) received more attention and thus lots of CBIR approaches have been developed. CBIR retrieves relevant images from database using visual image contents. Commonly, CBIR approaches differ in exploring visual image contents and each visual image content exploits only one characteristics of the image such as texture, colour, shape, etc., and they must have high discrimination between images. The visual image contents are computed either locally or globally on the image. Since global level visual image contents fails to exploit sufficient discrimination, researchers are concentrated much on local level visual image contents. Further using single local level visual image content has limited discrimination capability, researchers combined various visual image contents for effective discrimination in CBIR. In the literature lots of CBIR approaches using local level visual contents are reported with varying degree of accuracy. For instance, co-occurrence of pixels and edgels is reported in [1] and [2] respectively; histogram of gradient location and orientation called as SIFT is reported in [3] and its variant is reported in [4], SURF is suggested in [5], LBP is introduced in [6], centre symmetric LBP is described in [7], co-occurrences of LBP is presented in [8], co-occurrence of centre symmetric LBP [9], LTP for medical, face and texture images [10], co-occurrence of LTP [11] is presented for MRI and CT images, autocorrelation based chordiagram image descriptor is reported for place recognition with illumination invariant

[12], Local wavelet pattern [13] for CT images, mixed intensity feature histogram [14], color difference histogram [15], etc are suggested for image retrieval. However, literature expose that single visual image contents are not sufficient for efficient image retrieval and have limited effects on discrimination, and thus fusion of color and edge histogram with Gabor features is used in [16], trous wavelet based correlogram and gradient structure is presented in [17], fusion of color information feature and LBP is introduced in [18], fusion of SIFT and LBP and fusion of HOG and LBP is reported by Yu et al [19], Fourier descriptor and moments invariants is used with SOM and support vector machine in [20], in [21] Murala et al., introduced local tetra patterns using horizontal and vertical directional pixels, microstructure descriptor that computes edge and texture details with underlying color is suggested by Liu et al., [22], combination of color autocorrelogram, edge histogram descriptor and compact micro-textures are used in [23], color and edge orientation autocorrelograms are combined with micro-texture in [24] for diverse medical image collections, Fourier descriptor is combined with k moments by Wu and Wu [25], mixture of color moments, LBP and canny edge features are used in [26], color histogram is combined with BDIPs and BVLCs in [27], co-occurrences of BDIPs and BVLCs is suggested in [28], covariance's of BDIPs and BVLCs is presented in [29], fusion of chordiogram image descriptor (CID), micro-textures and color autocorrelogram is suggested by Saravanan et al., [30] for heterogeneous medical images, Zhao et al., suggested an approach which exploits texture, color and shape details from the local structures based on trends along 0°, 45°, 90°and 135° orientations and coined it as multi-trend structure descriptor (MTSD) [31], MTSD is combined with fuzzy support vector machine for heterogeneous medical images in [32], Natarajan et al. described MTSD at micro-level in [33] which significantly increases the retrieval rate for histological images and also significantly robustness to lightning variations, a variant of MTSD is reported in [34], more discriminative geometrical, texture and spatial details are computed using autocorrelation based CID in [35] which is combined with SVM in [36] and combined with color autocorrelogram in [37], integration of color moments, moments invariants, ranklet histogram and co-occurrence matrix is presented in [38], which performs non-parametric statistical analysis at different resolution and different orientations on ranklet transformation to compute the ranklet coefficients based on relative order of pixels instead of their intensity values and the ranklet coefficients are used to compute the texture feature called ranklet histogram and co-occurrence matrix, Distribution of color ton (DCTon) is reported in [39] which is computed using dual tree complex wavelet transformation and singular value decomposition and it captures color and texture details of an image, Global correlation vector reported in [40] encompasses global correlation vector and directional global correlation vector and are taking the plus of structure element correlation and histogram statistics to describe color and texture details, Srivastava and Khare [41] reported LBP and legendre moments on discrete wavelet transform for improving the competence of retrieval, Bala and Kaur [42] performed XOR operation on texton and local binary pattern and coined it as local texton XOR patterns, Deep et al., [43] described directional local ternary quantized extrema pattern for biomedical images which extracts in-depth spatial information then the LBP and LTP operators because it computes spatial relationship of center pixel and its neighbors in local region as well along 0°, 45°, 90° and 135° using the ternary patterns of directional local extrema values of an image, local mesh ternary patterns reported in [44] is computed using the ternary patterns extracted from mesh patterns of the image, local quantized extrema quinary pattern is suggested for medical images in [45] which uses quinary patterns extracted from horizontal-vertical-diagonal-anti diagonal (HVDA7) structure of directional local extrema values of an image to compute much spatial details, local tri-directional pattern described by Verma and Raman [46] is a concatenation of magnitude patterns that are estimated from intensity differences along three different directions in local neighborhood, local directional gradient pattern is reported by Chakraborty et al.

[47] is low in dimension and has effective discriminative ability, [48] extracted texture, structural and multi-directional edge details from orthogonal Fourier – Mellin moments for medical images, [49] describes gray level co-occurrence matrix computed on 8 orientations with geometric shape features such as area, eccentricity, Euler number, Perimeter, Centroid, Convex area, Orientation etc. from the closed boundary and the moments on HSV for color image retrieval, etc., are reported for image retrieval.

Recently, we presented DRLBP with fuzzy k-NN then DRLBP and dominant edgels (DE) with self organizing map (SOM) for texture and histology images in [50] and [51] respectively. Though, [50] provides better results for texture and histology database, its competence need to be increased with robustness to rotation and thus in this paper, we employed dominant color descriptor (DCD) and shape features computed from moments of dominant edgels along with DRLBP and histogram of DE. The experiments evident that proposed integration of feature descriptor makes notable distinction between the images then the other approaches and also more resilient to rotation.

The rest of manuscript is prepared as: In section-2, extraction of texture, shape and color details are described; similarity and performance measures are described. Section 3 provides experimental results and discussion. The conclusion is discussed in section 4.

2. Proposed Feature Extraction Method

In Figure 1, the architecture of proposed image retrieval system (IRS) is depicted and the feature extraction methodology adopted in the proposed IRS is explained as follows.

2.1.Local Binary Pattern

In an image I of M x N size, every pixel is considered as center pixel to encode local pattern among center and its neighbor's pixel. Neighbor pixels at distance or radius 1 are compared with center, depends on higher or lower value of neighbor pixel than center, a binary label is assigned for neighbors and are multiplied by corresponding weights followed by summation provides local binary pattern. The local binary map is constructed by combining LBPs of all center pixels of an image [1]. The LBP [1] is delineated as

$$LBP_{N,R} = \sum_{p=1}^{N} T(I_p - I_c) \times 2^{p-1} \tag{1}$$

Where N, R, I_p and I_c signifies number of neighbors, radius around center pixel (I_c), pth neighbor pixel and center pixel respectively and T(p)=1 if $p \geq 0$ else 0.

$$H(L)\Big|LBP = \sum_{m=1}^{M} \sum_{n=1}^{N} P(LBP(m,n), L);\ L \in [0, \left(2^N - 1\right)] \tag{2}$$

Where H (L) signifies histogram for LBP.

2.2.Dominant Rotated LBP

In [6], Mehta and Egiazarian delineated DRLBP as

$$DRLBP_{N,D} = \sum_{p=1}^{N} T(I_p - I_c) \times 2^{\mathrm{mod}(p-D,p)} \tag{3}$$

Where $2^{\mathrm{mod}(p-D,p)}$ and D signifies weight and dominant direction. The weight is depends on D. The maximum difference among center and neighbor pixels is marked as index for dominant direction [20] and is

$$D = \underset{p \in (0,1,.,.,.,p-1)}{\arg\max} \left|(I_p - I_c)\right| \tag{4}$$

The DRLBP is calculated by assigning weights from the index of dominant direction in circular mode and the run of weights remains as in LBP. In DRLBP, fixed arrangement is not followed in assigning weights and it varies depends on maximum variation among center and its neighbors [20].

2.3.Histogram of Dominant Edgels

Since Sobel operator [16] is used extensively for edge identification, we incorporated it in the proposed IRS. Later, to decrease the computation cost and to attain robustness against illumination and view point, we computed dominant boundary pixels i.e. Dominant edgels (DE), which are higher in gradient magnitudes and robust to illumination and rotation invariant because DE remains dominant while lighting or view position vary. Thus, we define the number of DE as

$$N_{DE} = p.N_E \tag{5}$$

where p exemplifies the proportion of DE and N_E is the number of edgels identified by Sobel operator. In the proposed IRS, p determines the size of DE and we have chosen varies choices for p such as 5%, 10%, 15%, 20%, 25% and 30%, and we experimentally discovered that p=15% gives better results against illumination variation and also decreases time cost enormously. In the experiments, when we increase p from 0% to 15%, precision increases gradually. Thereafter, precision is stable. Therefore, we set p=15% in the proposed IRS.

2.4.Moments of Dominant Edgels

In addition to the histogram of dominant edgels, we also computed the low and high order moments of dominant edgels namely mean, standard deviation, skewness and kurtosis and are described as follows.

The location of distribution of dominant edgels is estimated as

$$\mu_{DE} = \frac{1}{N_{DE}} \sum_{i=1}^{N_{DE}} DE_i \tag{6}$$

where N_{DE} signifies number of dominant edgels. The standard deviation measures the spread of dominant edgels distribution and is

$$\sigma = \sqrt{\frac{1}{N_{DE}} \sum_{i=1}^{N_{DE}} (DE_i - \mu_{DE})^2} \tag{7}$$

The skewness is a measure of asymmetry of distribution of dominant edgels about the location of distribution of dominant edgels i.e., it measures the amount and direction of asymmetry of distribution of dominant edgels and it falls into three categories namely fairly, moderately and highly skewed and it is estimated as in Eq. (8)

$$\text{Skewness} = \sum_{i=1}^{N_{DE}} \frac{(DE_i - \mu_{DE})^3}{N_{DE}\sigma^3} \tag{8}$$

The kurtosis measures the taildness in the distribution of dominant edgels i.e., it measures the tall and sharpness in the distribution of dominant edgels and it falls into three categories namely mesokurtic, leptokurtic and platykurtic and are representing sharply, medium and flattest peaked distributions respectively and is estimated as in Eq. (9)

$$\text{Kurtosis} = \sum_{i=1}^{N_{DE}} \frac{(DE_i - \mu_{DE})^4}{N_{DE}\sigma^4} \tag{9}$$

2.5.Dominant Color Descriptor

The DCD is introduced by MPEG-7 and it exploits number of dominant colors (N_c), percentage (P_i), spatial homogeneity (S_i) and variance (V_i) of each dominant color. The DCD is extensively employed in CBIR because it provides compact and more effective color information and is delineated as

$$F_c = \{D_i, P_i, S_i, V_i\} where i = 1,2.,.,., N_c \tag{10}$$

Where D_i is ith dominant colors. In DCD, V_i is optional one and S_i is set to 0. In accordance with [23], we fixed $N_c = 8$ because large color numbers leads to complexity in computation and unimportant dominant colors in large color numbers may introduce noise, small color numbers may fails to provide accurate representation of the image.

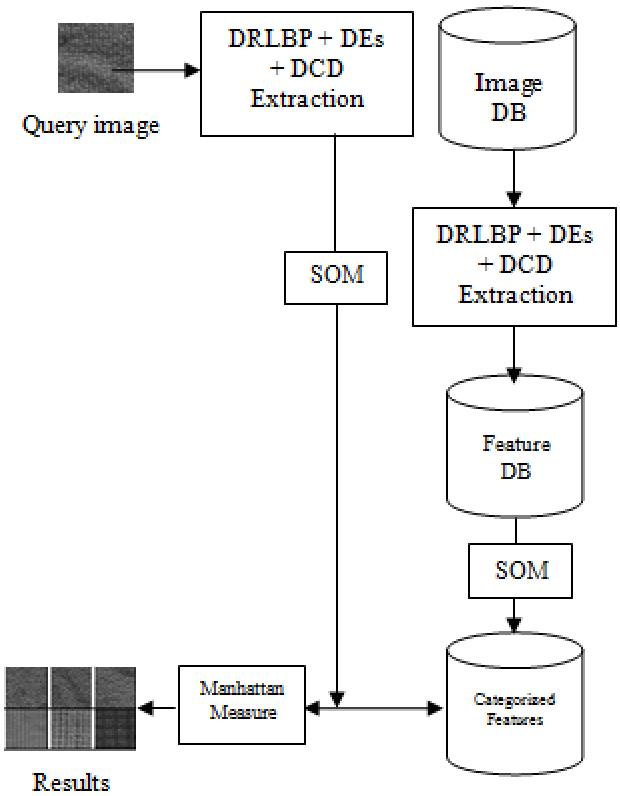

Figure 1. Flowchart of proposed IRS

2.6.Self Organizing Map

Over the decade, researchers employed artificial neural networks (ANNs) for classification owing to its precision [50] Although many ANNs are available, SOM [50] is incorporated in many applications because of its ability to organizing large and complex data sets and it preserves topological relations in the data which exploits underlying structure of data and is an intrinsic feature to the problem. SOM is a feed-forward network and it maps high dimensional data patterns in input space to n-dimensional output space based on competitive and cooperation learning which falls on unsupervised learning category. In SOM, number of nodes in input is decided by the dimension of input vector, connection exists among input nodes and neurons in computational layer and connection does not exist among the neurons in computational layer.

Let I be input vectors and number of input vectors in I are $\{I_1, I_2,.,., I_N\}$. Initially weights (W_{ji}) are assigned randomly with small value (in the range 0 to 1) for each connection between input nodes i and neurons j where $j = 1,2,.,.,., M$ and M is number of neurons and usually it is less than or equal to half of number of classes in the datasets. The SOM algorithm is described as follows
For each input vectors in training dataset

1. Input vector is selected randomly from the training data.
2. Weights are adjusted using competitive learning when training progress and the winning neuron (the neurons whose weight vector become most similar to input vector) for each input vector is computed using the discriminant function such as Euclidean distance. However, in the proposed IRS, instead of Euclidean, we implemented Manhattan distance as discriminant function owing to its effectiveness and less computation cost and is described as follows for neuron j and input pattern I in Eq. [11].
$$D_j(I) = \sum_{i=1}^{N}(I_i(t) - W_{ji}(t)) \tag{11}$$
where $I_i(t)$ - i[th] input of I at time t and $W_{ji}(t)$ - weight vector of jth neuron and ith input vector at time t. The winning neuron is coined as best matching unit and is computed as follows
$$\text{WN=arg min } \{ D_j(I), \text{ j=1,2,.,.,.,N}\} \tag{12}$$
3. The neighborhood of winning neuron is decided with the help of concentric squares or hexagons or any other polygon shapes or functions such as Maxican Hat, Gaussian, etc., Generally, the neighborhood function offers cooperation process among the winner and its neighbor and it is designed such that the weights of winning one has global maxima and the neurons close to winning one are scaled towards winning one and the neurons far away from winning one are scaled towards least i.e. more closer neighbors are excited more than the neighbors at furthest distance. In SOM, this weight adjustment is coined as adaption process. Initially, the size i.e. radius of neighborhood function is large and start to decrease when training progress and thus neighbors which are far away from the winning neuron are eliminated. The weight adjustment equation in SOM is as follows
$$W_{ji}(t+1) = W_{ji}(t) + \eta(t).h_{ji}(t).(I_i - W_{ji}(t)) \tag{13}$$
where $\eta(t)$ is learning rate which explains how much the weights need to be adjusted and is given as
$$\eta(t) = \eta_0\left(1 - \frac{t}{T}\right) \tag{14}$$
where η_0 symbolizes the initial value of η and usually η_0=1, and T symbolizes maximum time of iteration. Learning rate will converge to 0 after T. In the proposed work, we incorporated Gaussian as neighborhood function. As aforementioned, during the learning process, the neighborhood function measures the degree of cooperation with the winner. The Gaussian neighborhood function is given as follows
$$h_{ji}(t) = \exp\left[\frac{D_j(I)^2}{2\sigma^2(t)}\right] \tag{15}$$

where t is time or epoch, $D_j(I)$ symbolizes the Euclidean distance of neuron j and input pattern I and σ is width of Gaussian function. To get the best learning rate, σ is decreased gradually during learning progress. In Eq.(16), $\sigma(t)$ is described as

$$\sigma(t) = \sigma_0 \exp\left(-\frac{t}{\tau}\right) \tag{16}$$

Where σ_0 is initial value of σ and τ is time constant.

4. End For

Through steps 1 to 4, a feature map in SOM is created.

2.7.Measure of likeness

Similarity metrics measure the divergence among input images and the images in database. Since it filtering out irrelevant images, it becomes an important component of any image retrieval system and thus it must be chosen more cautiously. It is revealed from the literature that Manhattan measure is more effective and its computational complexity is less among the other metrics. Therefore, it is employed in the proposed system [32].

Manhattan measure uses sum of absolute differences of variables [32] and also described as a measure among two points in Euclidean space with fixed Cartesian coordinate system [32]. The Manhattan measure among two images is defined as

$$S\left(I^q, I^t\right) = \sum_{i=1}^{k}\left(I_i^q - I_i^t\right) \tag{17}$$

Where, I_i^q and I_i^t - query and target image feature descriptors respectively and k - size of combined feature descriptor. After computing divergence among all database and input images, the values obtained by Manhattan metric are sorted out in ascending manner. Accordingly, database images are displayed to user based on top n most Manhattan metric results.

2.8.Performance estimation

We measured the performance of retrieval rate using more familiar measures precision (P) and recall (R). The accuracy of retrieval out of top k retrieved images is computed using P and accuracy with respect to total number of relevant images in the database is computed using R based on similarity value with query images. The P and R is defined as in [32-37]

$$\Pr ecision = \frac{I_N}{N} \tag{18}$$

$$\text{Re}\,call = \frac{I_N}{M} \tag{19}$$

where I_N, N and M are number of relevant images retrieved, total number of images retrieved and total number of relevant images in the database respectively. The average P [32-37] for a given query image (I) is defined as an average of P values of top N relevantly retrieved images and is given as

$$\mu_{P(I)} = \frac{1}{N}\sum_{i=1}^{N} P \tag{20}$$

The mAP [32-37] is defined as average P for all the input images and is expressed as follows

$$mAP = \frac{1}{N_I}\sum_{k=1}^{N_I} \mu_{P(I)} \tag{21}$$

where N_I designates total number of input images.

3. Experimental Results

In the experiments, we used Outex 10 and 12, KTH-TIPS, KTH-TIPS ROT and histology datasets are used and are described as follows. The example texture and histological images from experimental datasets are depicted in Figure 2.

3.1. Outex 10 Dataset

The Outex 10 dataset [6] has 4320 texture images of 24 categories. The textures are acquired under constant lightening setting and nine dissimilar orientations that is $(0^\circ,5^\circ,10^\circ,15^\circ,30^\circ,45^\circ,60^\circ,75^\circ,90^\circ)$. The dataset contains 20 images for each angle in each category. As described in [6], images in 0° of all categories i.e. 480 images are used in training and images in remaining orientations are used in testing phase i.e. 3840 images.

3.2. Outex 12 Dataset

The Outex 12 dataset [6] has 9120 texture images of 24 categories. The textures are acquired under varies lightening setting and rotations. As in [6], we incorporated 8640 and 480 texture images in training and testing phases.

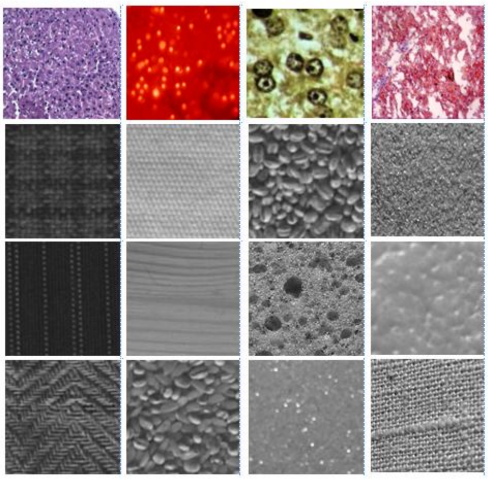

Figure 2.Example images from experimental texture and histological dataset

3.3. KTH-TIPS Dataset

The dataset has 10 categories of textures and each category has 81 texture images and the images are acquired under 9 varies scales, 3 varies poses and 3 varies illuminations circumstances. As described in [6], we used 40 images of each category in training and remaining are in testing phases.

3.4. KTH-TIPS ROT Dataset

The texture images in KTH-TIPS are randomly rotated between 0° to 360° degrees and the images are cropped for 100x100 size from their center and are used in experiments as in [6]. As in [6], we randomly selected 40 texture images in training phase and remaining are used in testing phase.

3.5. Histology Dataset

The dataset used in [32] has medical images of various modalities. Since our interest is on histological images, we segregate it into separate dataset which consists of 1708 images of 16 categories and the images are acquired using various histological stains.

ISSN: 2233-7857 IJFGCN

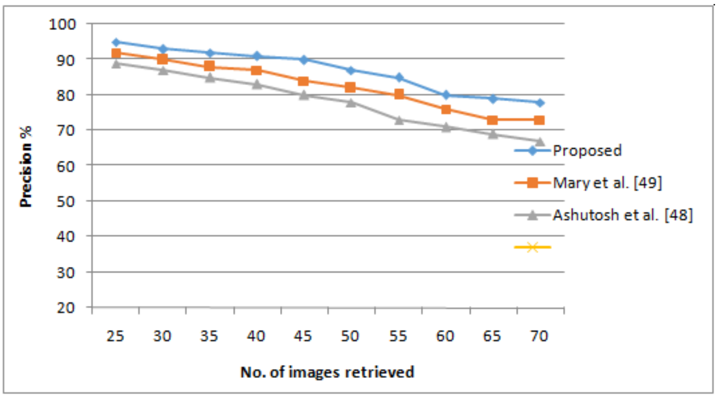

Figure 3. P Vs R for proposed and existing approaches for Outex 10 dataset

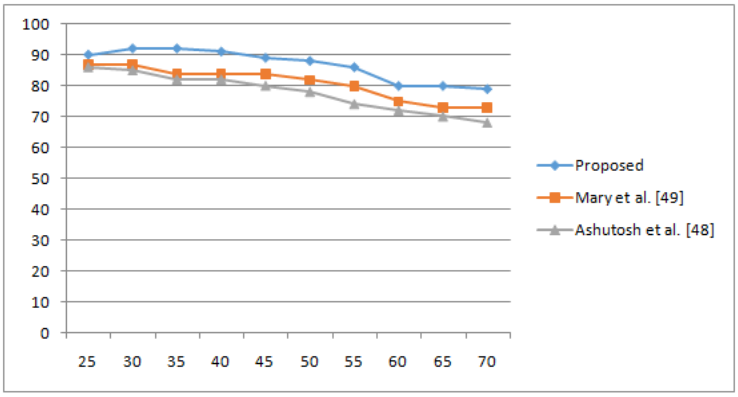

Figure 4. P Vs R for proposed and existing approaches for Outex 12 dataset

In this paper, we computed Fourier-Mellin moments [48], gray level co-occurrence matrix computed on 8 orientations with geometric shape features such as area, eccentricity, Euler number, Perimeter, Centroid, Convex area, Orientation etc. from the closed boundary and the moments on HSV [49] and the proposed combination of DRLBP, histogram of dominant edgels, moments of dominant edgels and dominant color descriptor for all the images in the benchmark datasets and are stored in corresponding feature descriptor dataset and the search operation is performed in the feature descriptor space using SOM with Manhattan metric. Since ultimate aim is high accuracy with rotation and scaling invariance, we have selected the features more carefully in the proposed IRS.

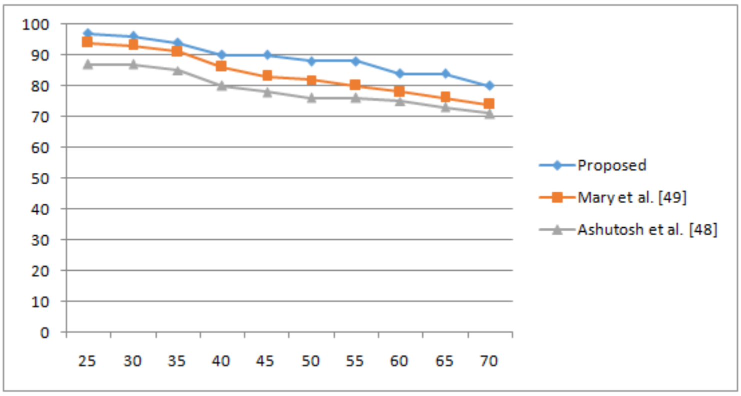

Figure 5. P Vs R for proposed and existing approaches for KTH-TIPS dataset

International Journal of Future Generation Communication and Networking
Vol. 13, No. 1, (2020), pp. 57-70

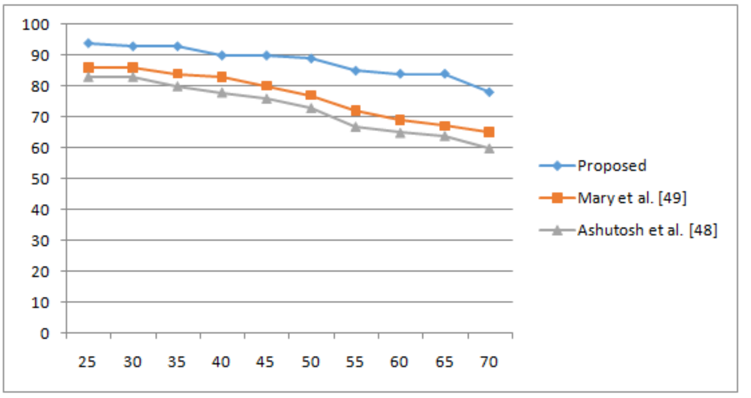

Figure 6. P Vs R for proposed and existing approaches for KTH-TIPS ROT dataset

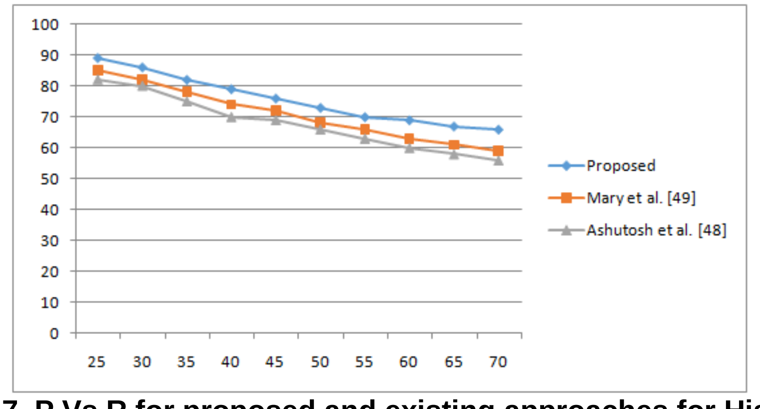

Figure 7. P Vs R for proposed and existing approaches for Histology dataset

Table 1. mAP for top 10 images retrieved by [48] [49], and proposed IRS on Outex 10, Outex 12, KTH-TIPS, KTH-TIPS ROT, Histology datasets

Datasets	Ashutosh et al. [48]	Mary et al. [49]	Proposed IRS
Outex 10	81.11	83.88	87.22
Outex 12	80.91	82.90	86.90
KTH-TIPS	82.01	84.06	87.90
KTH-TIPS ROT	80.12	82.10	86.84
Histology dataset	69.23	72.49	78.45.

Query Retrieval result

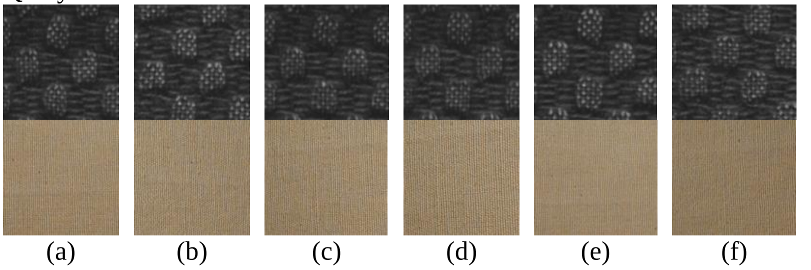

(a) (b) (c) (d) (e) (f)

Figure.8. Example query image and top 4 retrieval results of proposed IRS for benchmark datasets

To assess the competence of proposed IRS, we utilized average P and average R. The proposed IRS is compared with the existing systems [48] and [49]. The P Vs R graph for proposed IRS and existing systems are illustrated in Figure 3 - 7 for Outex 10, Outex 12, KTH-TIPS, KTH-TIPS ROT, Histology datasets respectively. Figure 3 - 7 illustrates that performance of proposed IRS i.e., the combination of DRLBP, histogram of dominant edgels, moments of dominant edgels and dominant color descriptor with SOM and Manhattan measure is significantly superior to conventional approaches [48] and [49] for top N returned images. The results of proposed IRS, existing systems using Fourier-Mellin moments [48] and the system based on gray level co-occurrence matrix computed on 8 orientations with geometric shape features and moments on HSV [49] are depicted in Table 1 for top k returned images and the accuracy are 87.22%, 81.11% and 83.88%; 86.90%, 80.91% and 82.90%; 87.90%, 82.01% and 84.06%; 86.84%, 80.12% and 82.10%; 78.45%, 69.23%, 72.49%. for Outex 10, Outex 12, KTH-TIPS, KTH-TIPS ROT, Histology datasets respectively. The mAP for top 10 images retrieved by [48], [49] and proposed IRS on Outex 10, Outex 12, KTH-TIPS, KTH-TIPS ROT, Histology datasets are represented in Table 2 for randomly selected categories of images.

Table 2. Randomly selected class wise mAP for top 10 images retrieved by Ashutosh et al. [48], Mary et al. [49] and proposed IRS on benchmark datasets

Class	mAP		
	Ashutosh et al. [48]	Mary et al. [49]	Proposed IRS
Canvas022	82,.00	84.80	87.00
Canvas033	81.19	83.01	86.34
Canvas003	81.22	83.45	86.90
Canvas001	80.34	82.19	86.10
Carpet004	79.90	83.90	86.01
Tile005	78.76	82.18	87.02
Tile006	82.21	83.15	85.92
Linen	78.90	80.45	85.32
Sandpaper	79.22	83.21	86.39
Sponge	80.14	82.19	87.51
Breast–Hematoxylin & Eosin- Benign	69.67	71.90	76.90

Table 3. Time taken (milli seconds) by Ashutosh et al. [48], Mary et al.[49] and the proposed IRS

Methods	Time cost (ms)
Ashutosh et al. [48]	18
Mary et al. [49]	33
Proposed IRS	31

Table 4. Classification accuracy of SOM with various discriminant functions

Datasets	SOM		
	Manhattan	Euclidean	Minkowski
Outex 10	70.13	69.99	67.31
Outex 12	70.10	69.84	67.25
KTH-TIPS	66.12	65.78	64.22
KTH-TIPS ROT	67.20	66.90	65.10
Histology dataset	58.11	57.89	57.09

In the experiments, we also evaluated the competence of proposed IRS using Euclidean, Manhattan and Minkowski distances as a discriminant function of SOM respectively and the results proven that Manhattan notably decreases the computation cost of SOM and considerably increases the classification accuracy of SOM and the results are depicted in Table 4.

4. Conclusion

In this work, the rotationally invariant color, texture and shape descriptor is proposed. The DCD estimates the color information, distribution of dominant edgels, low and high order moments of dominant edgels represents the shape information, and DRLBP estimates the texture details. The proposed system merges the computed features and are classified using SOM. In SOM, we incorporated Manhattan distance as discriminant function. The likenesses of query and dataset images are measured using Manhattan distance. The results obviously shown evidence that proposed system for retrieval of images is notably superior to existing systems. In future, the accuracy of proposed system can be extended by computing the proposed feature descriptors from wavelet domain.

References

[1] R. M. Haralick, K. Shanmugam, and I. Dinstein, “Textural Features for Image Classification”, IEEE Trans. on Systems, Man, and Cybernetics, Vol. SMC-3, No.6, (1973), pp.610-621.

[2] J. Zhang, G.l. Li, S.W. He, Texture-based image retrieval by edge detection matching GLCM, in: 10th IEEE International Conference on High Performance Computing and Communications, (2008), pp. 782–786.

[3] D.G. Lowe, Distinctive image features from scale-invariant keypoints, Int. J. Comput. Vis. 60 (2004) 91–110.

[4] K. Mikolajczyk, C. Schmid, A performance evaluation of local descriptors, IEEE Trans. Pattern Anal. Mach. Intell. 27 (2005) 1615–30.

[5] H. Bay, A. Ess, T. Tuytelaars, L. Van Gool, Speeded-up robust features (SURF), Comput. Vis. Image Underst. 110 (2008) 346–359.

[6] T. Ojala, M. Pietikäinen, D. Harwood, A comparative study of texture measures with classification based on featured distributions, Pattern Recognit. 29 (1996) 51–59.

[7] M. Heikkilä, M. Pietikäinen, C. Schmid, Description of interest regions with local binary patterns, Pattern Recognit. 42 (2009) 425–436.

[8] Vahid Naghashi, Co-occurrence of adjacent sparse local ternary patterns: A feature descriptor for texture and face image retrieval, Optik 157 (2018) 877–889.

[9] Manisha Verma, Balasubramanian Raman, Center symmetric local binary co-occurrence pattern for texture, face and bio-medical image retrieval, Journal of Visual Communication and Image Representation, Volume 32, (2015), Pages 224-236.

[10] X. Tan and B. Triggs, Enhanced local texture feature sets for face recognition under difficultlighting conditions, IEEE Transactions on Image Processing 19 (6) (2010) 1635–1650.

[11] Subrahmanyam Murala, Q.M. Jonathan Wu, Local ternary co-occurrence patterns: A new feature descriptor for MRI and CT image retrieval, Neurocomputing, (2013), 119: 399–412.

[12] A.Saravanan, S.Sathiamoorthy, Autocorrelation based Chordiogram Image Descriptor for Image Retrieval, 4th International Conference on Communication and Electronics Systems (ICCES 2019), July 17-19, (2019), PPG Institute of Technology, Coimbatore.

[13] S.R. Dubey, S.K. Singh, R.K. Singh, Local wavelet pattern: a new feature descriptor for image retrieval in medical CT databases, IEEE Trans. Image Process. (2015) 24 (12) 5892–5903.

[14] Yi Yang, Fajie Duan, Ling Ma, A rotationally invariant descriptor based on mixed intensity feature histograms, Pattern Recognition 76 (2018) 162–174.

[15] G.H. Liu, J.Y. Yang, Content-based image retrieval using color difference histogram, Pattern Recogn. (2013), 46 (1) :188–198.

[16] Hossein Nezamabadi-pour, Ehsanollah Kabir, Concept learning by fuzzy k-NN classification and relevance feedback for efficient image retrieval, Expert Systems with Applications, (2009), 36: 5948–5954.

[17] M. Agarwal, R. P. Maheshwari, Á trous Gradient Structure Descriptor for ContentbasedImage Retrieval, International Journal of Multimedia Information Retrieval.1(2) (2012) 129-138.

[18] L.K. Pavithra, T. Sree Sharmila, An efficient framework for image retrieval using color, texture and edge features, Computers and Electrical Engineering , (2017), 1–14

[19] J. Yu, Z. Qin, T. Wan, X. Zhang, Feature integration analysis of bag-of-featuresmodel for image retrieval, Neurocomputing. 120, (2013), 355-364.

[20] Wai-Tak Wong, Frank Y. Shih, Jung Liu, Shape-based image retrieval using support vector, machines, Fourier descriptors and self-organizing maps, Information Sciences, 177, (2007), 1878–1891.
[21] S. Murala, R.P. Maheshwari, R. Balasubramanian, Local tetra patterns: anew feature descriptor for content-based image retrieval, IEEE Trans. Image Process. 21(5) (2012) 2874–2886.
[22] Liu G.H., Li, Z.Y., Zhang, L., Xu. Y., Image retrieval based on micro-structure descriptor. Pattern Recognition. (2011), 44(9): 2123-2133.
[23] K.Seetharaman, S.Sathiamoorthy,Color image retrieval using statistical model and radial basis function neural network, Egyptian Informatics Journal, (2014), 15(1): 59-68.
[24] K.Seetharaman, S.Sathiamoorthy, A Unified Learning Framework for Content Based Medical Image Retrieval Using a Statistical Model, Journal of King Saud University - Computer and Information Sciences, (2016), 28 (1): 110-124.
[25] Y. Wu, Y. Wu, Shape based image retrieval using combining global and local shape features, in: 2nd International Congress on Image and Signal Processing, Tianjin, (2009).
[26] P. Srivastava, A. Khare, Integration of Wavelet Transform, Local Binary Patterns and Moments for Content-Based Image Retrieval, J. Vis. Commun. Image R. (2016), doi: http://dx.doi.org/10.1016/j.jvcir.2016.11.008.
[27] C. Singh, K. Preet Kaur, A Fast and Efficient Image Retrieval System Based on Color and Texture Features, J. Vis. Commun. Image R. (2016), doi: http://dx.doi.org/10.1016/j.jvcir.2016.10.002
[28] M. Bennet Rajesh, S.Sathiamoorthy, Covariance Descriptor with a Statistical Measure of Divergence for Image Retrieval, 4th International Conference on Communication and Electronics Systems (ICCES 2019), July 17-19, (2019), PPG Institute Of Technology, Coimbatore.
[29] M. Bennet Rajesh, S.Sathiamoorthy, Co-occurrence of Edges and Valleys for Content Based Image retrieval, 4th International Conference on Communication and Electronics Systems (ICCES 2019), July 17-19, (2019), PPG Institute Of Technology, Coimbatore.
[30] A.Saravanan , M. Natarajan and S. Sathiamoorthy, A Novel Hybrid Framework for Medical Image Retrieval, Asian Journal of Engineering and Applied Technology, Vol. 7, No.1, Jan-June 2018, pp 37-41.
[31] Meng Zhao, Huaxiang Zhang, Jiande Sun, A novel image retrieval method based on multi-trend structure descriptor, J. Vis. Commun. Image R., (2016), 38: 73–81.
[32] M. Natarajan, S. Sathiamoorthy, Heterogeneous Medical Image Retrieval using Multi-Trend Structure Descriptor and Fuzzy SVM Classifier, International Journal of Recent Technology and Engineering (IJRTE) ISSN: 2277-3878, Volume-8 Issue-3, pp.3958-3963, September (2019).
[33] M. Natarajan, S. Sathiamoorthy, Multi-Trend Structure Descriptor At Micro-Level For Histological Image Retrieval, International Journal of Recent Technology and Engineering (IJRTE) ISSN: 2277-3878, Volume-8 Issue-3, pp. 7539-7543, September (2019).
[34] Sathiamoorthy, S., Natarajan, M. An efficient content based image retrieval using enhanced multi-trend structure descriptor. SN Appl. Sci. 2, 217 (2020) doi:10.1007/s42452-020-1941-y.
[35] A.Saravanan, S.Sathiamoorthy, Autocorrelation based Chordiogram Image Descriptor for ImageRetrieval, 4th International Conference on Communication and Electronics Systems (ICCES 2019), July 17-19, (2019), PPG Institute of Technology, Coimbatore.
[36] A.Saravanan, S.Sathiamoorthy, Image Retrieval using Autocorrelation Based Chordiogram Image Descriptor and Support Vector Machine, International Journal of Recent Technology and Engineering (IJRTE) ISSN: 2277-3878, Volume-8 Issue-3, pp. 6019-6023, September 2019.
[37] A.Saravanan, S.Sathiamoorthy, Integration of Statistical Based Texture and Color Feature for Medical Image Retrieval, International Journal of Recent Technology and Engineering (IJRTE) ISSN: 2277-3878, Volume-8 Issue-3, pp. 5584-5588, September 2019.
[38] Soumya Prakash Rana, Maitreyee Dey, Patrick Siarry, Boosting content based image retrieval performance through integration of parametric & nonparametric approaches, J. Vis. Commun. Image R. 58 (2019) 205–219.
[39] M. Rahimi, M.E. Moghaddam, A content-based image retrieval system based on color ton distribution descriptors, Signal Image Video Process. 9 (2015) 691–704.
[40] L. Feng, J. Wu, S. Liu, H. Zhang, Global correlation descriptor: a novel image representation for image retrieval, J. Vis. Commun. Image Represent. 33 (2015) 104–114.
[41] P. Srivastava, A. Khare, Integration of wavelet transform, local binary patterns and moments for content-based image retrieval, J. Vis. Commun. Image Represent. 42 (2017) 78–103.
[42] Anu Bala, Tajinder Kaur, Local texton XOR patterns: A new feature descriptor for content based image retrieval, Engineering Science and Technology, an International Journal 19 (2016) 101–112.
[43] G. Deep, L. Kaur, S. Gupta, Local mesh ternary patterns: a new descriptor forMRI and CT biomedical image indexing and retrieval, in: Computer Methodsin Biomechanics and Biomedical Engineering: Imaging & Visualization, 2016,pp. 1–15, http://dx.doi.org/10.1080/21681163.2016.1193447.
[44] G. Deep, L. Kaur, S. Gupta, Local quantized extrema quinary pattern: a newdescriptor for biomedical image indexing and retrieval, Comput. MethodsBiomech. Biomed. Eng. Imaging Vis. (2017) 1–17, http://dx.doi.org/10.1080/21681163.2017.1344933.
[45] M. Verma, B. Raman, Local tri-directional patterns: a new texture featuredescriptor for image retrieval, Digit. Signal Process. 51 (2016) 62–72.

[46] M.Verma, B. Raman, Local neighborhood difference pattern: a new feature descriptor for natural and texture image retrieval, Multimedia. Tools and Applications.(2017) 1–24, http://dx.doi.org/10.1007/s11042-017-4834-3.
[47] S. Chakraborty, S.K. Singh, P. Chakraborty, Local directional gradient pattern: alocal descriptor for face recognition, Multimed. Tools Appl. (2017) 1–16,http://dx.doi.org/10.1007/s11042-015-3111-6.
[48] Ashutosh Aggarwal, Suchita Sharma, Karamjeet Singh, Harpreet Singh,Sunil Kumar, A new approach for effective retrieval and indexing of medical images, Biomedical Signal Processing and Control 50 (2019) 10–34.
[49] Mary I Thusnavis Bella, A. Vasuki, An efficient image retrieval framework using fused information feature, Computers and Electrical Engineering 75 (2019) 46–60.
[50] S. Sivakumar and S. Sathiamoorthy, "Image Retrieval Using Fuzzy k-NN on Dominant Rotated Local Binary Patterns, (2019) International Conference on Smart Systems and Inventive Technology (ICSSIT), Tirunelveli, India, (2019), pp. 806-812. doi: 10.1109/ICSSIT46314.2019.8987898.
[51] S.Sivakumar, S.Sathiamoorthy, Dominant Feature Descriptors With Self Organising Map for Image Retrieval, 2nd International Conference on Computer Networks, Big Data and IoT [ICCBI 2019], 9-20, December 2019, Vaigai College of Engineering, Madurai, India.

Authors

S.Sivakumar, received M.C.A degree from Bharathidasan University and M.Phil degree from Annamalai University, India. He joined in the Annamalai University in the year 2004. At present he is with the Department of Computer and Information Science, Annamalai University. He has almost 15 years of teaching experience. He is currently pursuing Ph.D degree in the Department of Computer and Information Science, Annamalai University. His research interests include Digital image processing and Content-based image retrieval.

S.Sathiamoorthy, received B.Sc degree in Physics from University of Madras, M.C.A degree from Bharathidasan University and M.Phil as well as Ph.D. from Annamalai University, India. In the year 2001, he joined in the Department of Computer Science and Engineering, Annamalai University and also served in the Computer Science and Engineering Wing of Directorate of Distance Education and Department of Computer and Information Science, Annamalai University. At present, he is Assistant Director (Controller of Examinations), Tamil Virtual Academy, Information Technology Department of Tamil Nadu Government, India. He has almost 19 years of teaching experience. Currently he is working on Pattern recognition, Pattern analysis, Image retrieval and classification. His research interests include Machine learning algorithms and Medical image analysis. He has published more than 30 papers in various International journals and more than 20 papers in National and International conferences. He has been on the reviewing and editorial board of many reputed journals.